Experimental Study of Particle Structuring in Vertical Stratifying Films from Latex Suspensions

E. S. Basheva, K. D. Danov, and P. A. Kralchevsky*

Laboratory of Thermodynamics and Physico-chemical Hydrodynamics, Faculty of Chemistry, University of Sofia, 1126 Sofia, Bulgaria

Received February 12, 1997. In Final Form: May 6, 1997[⊗]

Two independent interference methods, based on wavelength and intensity measurements, are applied to establish the type of packing of latex particles contained within vertical stratifying films. The films are formed in a ring-shaped frame after its pulling out from a latex suspension. They exhibit a stepwise profile, which appears as a set of parallel stripes of uniform intensity varying from stripe to stripe. Both interference methods allow a study of the stratification phenomenon "*in vivo*", i.e. during the process of film drainage. To fit the data from each of these two methods, we assume a given type of particle packing, in our case hexagonal or tetragonal, and then we check which type is consistent with the data. In all cases the data indicate the presence of *hexagonal* packing and do not agree with tetragonal packing. The developed technique can be further applied to examine the particle structuring in stratifying films containing smaller particles, such as surfactant micelles or protein globules. The results can be helpful for a deeper understanding of the stratification phenomenon and the underlying oscillatory structural forces.

1. Introduction

In the beginning of this century Johnnott[1] and Perrin[2] observed that soap films decrease their thickness by several stepwise transitions. The phenomenon was called "stratification". Bruil and Lyklema[3] and Friberg *et al.*[4] studied systematically the effect of ionic surfactant and electrolyte on the occurrence of the stepwise transitions. Kruglyakov *et al.*[5,6] reported the existence of stratification with emulsion films. Keuskamp and Lyklema[7] anticipated that some oscillatory interaction between the film surfaces must be responsible for the observed phenomenon.

Some authors[6,8] suggested that a possible explanation of the phenomenon can be the formation of surfactant lamellar liquid-crystal structure inside the film. Such lamellar micelles are observed to form in surfactant solutions, however, at concentrations much higher than those used in the experiments with stratifying films; this makes the explanation with lamellar liquid crystals problematic. Nikolov *et al.*[9−11] observed stratification not only with micellar surfactant solutions but also with suspensions of latex particles of micellar size. The stepwise changes in the film thickness were approximately equal to the diameter of the spherical particles contained in the foam film.[9−14] The experimental observations show that stratification is observed always, when spherical colloidal particles are present in the film at sufficiently high concentration. The observed multiple stepwise changes in the film thickness (Figure 1) can be attributed to the layer-by-layer thinning of a colloid-crystal-like structure inside the film.[9] The mechanism of stratification was studied theoretically in ref 15, where the appearance and expansion of black spots in horizontal stratifying films was described as a process of condensation of vacancies in a colloid crystal of ordered micelles within the film.

In fact, the stepwise transitions are a manifestation of the oscillatory structural forces in the thin liquid films. Such structural forces due to micelles and microemulsion droplets were directly measured by means of a surface force balance by Richetti *et al.*[16,17] The stable branches of the oscillatory disjoining pressure isotherm have been measured by Bergeron and Radke[18,19] with micellar solutions by means of a version of the experimental cell of Mysels.[20]

In general, oscillatory structural forces appear in two cases: (i) in thin films of pure solvent between two smooth *solid* surfaces and (ii) in thin liquid films containing colloidal particles (including protein macromolecules and surfactant micelles). In the first case the oscillatory forces are called the "solvation forces";[21,22] they could be important for the short-range interactions between *solid* particles in dispersions. In the second case, the structural forces affect the stability of foam and emulsion films as well as the flocculation processes in various colloids. At higher particle concentrations the structural forces stabilize the liquid films and colloids.[10,14,23] At lower particle concentrations the structural forces degenerate into the *depletion attraction*, which is found to destabilize various dispersions.[22,24] In all cases the oscillatory structural forces appear when monodisperse spherical (in some cases ellipsoidal or cylindrical) particles are confined between

* Author to whom correspondence should be addressed.

[⊗] Abstract published in *Advance ACS Abstracts,* July 1, 1997.

(1) Johnnott, E. S. *Philos. Mag.* **1906**, *70*, 1339.
(2) Perrin, R. E. *Ann. Phys.* **1918**, *10*, 160.
(3) Bruil, H. G.; Lyklema, J. *Nature* **1971**, *233*, 19.
(4) Friberg, S.; Linden, St. E.; Saito, H. *Nature* **1974**, *251*, 494.
(5) Kruglyakov, P. M. *Kolloidn. Zh.* **1974**, *36*, 160.
(6) Kruglyakov, P. M.; Rovin, Yu. G. *Physical Chemistry of Black Hydrocarbon Films;* Nauka: Moscow, 1978 (in Russian).
(7) Keuskamp, W.; Lyklema, J. *ACS Symp. Ser.* **1975,** *8*, 191.
(8) Manev, E.; Sazdanova, S. V.; Wasan, D. T. *J. Dispersion Sci. Technol.* **1984**, *5*, 111.
(9) Nikolov, A. D.; Wasan, D. T.; Kralchevsky, P. A.; Ivanov, I. B. In *Ordering and Organisation in Ionic Solutions;* Ise, N., Sogami, I., Eds.; World Scientific: Singapore, 1988.
(10) Nikolov, A. D.; Wasan, D. T. *J. Colloid Interface Sci.* **1989,** *133*, 1.
(11) Basheva, E. S.; Nikolov, A. D.; Kralchevsky, P. A.; Ivanov, I. B.; Wasan, D. T. In *Surfactants in Solution;* Mittal, K. L., Shah, D. O., Eds.; Plenum Press: New York, 1991; Vol. 12, p 467.
(12) Nikolov, A. D.; Kralchevsky, P. A.; Ivanov, I. B.; Wasan, D. T. *J. Colloid Interface Sci.* **1989,** *133*, 13.
(13) Nikolov, A. D.; Wasan, D. T.; Denkov, N. D.; Kralchevsky, P. A.; Ivanov, I. B. *Prog. Colloid Polym. Sci.* **1990,** *82*, 87.
(14) Wasan, D. T.; Nikolov, A. D.; Kralchevsky, P. A.; Ivanov, I. B. *Colloids Surf.* **1992,** *67*, 139.
(15) Kralchevsky, P. A.; Nikolov, A. D.; Wasan, D. T.; Ivanov, I. B. *Langmuir* **1990,** *6*, 1180.
(16) Richetti, P.; Kékicheff, P. *Phys. Rev. Lett.* **1992,** *68*, 1951.
(17) Parker, J. L.; Richetti, P.; Kékicheff, P. *Phys. Rev. Lett.* **1992,** *68*, 1955.
(18) Bergeron, V.; Radke, C. J. *Langmuir* **1992**, *8*, 3020.
(19) Bergeron, V.; Radke, C. J. *Colloid Polym. Sci.* **1995**, *273*, 165.
(20) Mysels, J. *J. Phys. Chem.* **1964**, *68*, 3441.
(21) Horn, R. G.; Israelachvili, J. N. *Chem. Phys. Lett.* **1980**, *71*, 192.
(22) Israelachvili, J. N. *Intermolecular and Surface Forces*; Academic Press: London, 1992.
(23) Koczo, K.; Nikolov, A. D.; Wasan, D. T.; Borwankar, R. P.; Gonsalves, A. *J. Colloid Interface Sci.* **1996**, *178*, 694.

S0743-7463(97)00145-5 CCC: $14.00

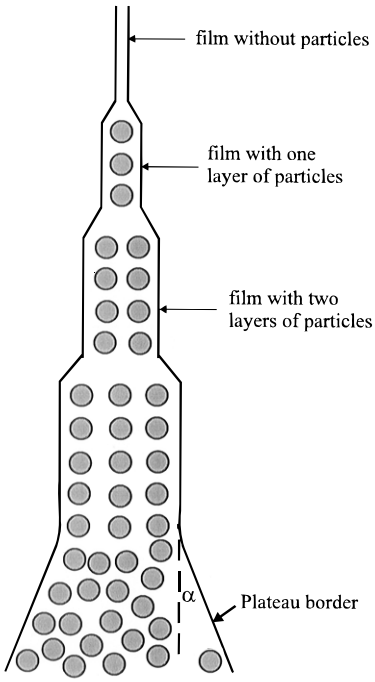

Figure 1. Sketch of a vertical stratifying film containing monodisperse colloid particles. The stepwise profile of the film is due to the variation in the number of particle layers contained within the film.

the two surfaces of a thin film. The oscillations originate from the overlap of the structured zones at the two surfaces.[25−28] As the period of oscillations is close to the particle diameter, the structural forces are appropriately called the "volume exclusion forces" by Henderson,[29] who derived an explicit (though rather complex) formula for calculating these forces. Numerical simulations[30,31] and density-functional modeling[32] of the stepwise thinning of foam films are also available. Recently, a relatively simple semiempirical formula for the oscillatory structural component of disjoining pressure was proposed,[33] which was found to agree well with both theoretical predictions and measured contact angles of stratifying films from micellar surfactant solutions.[34] (The contact angle is subtended between the two extrapolated surfaces of the Plateau border encircling the film and is very sensitive to the energy of interaction between the two film surfaces; see ref 34.)

In spite of the good agreement between theory and experiment, a *direct* proof of the particle ordering within the stratifying films is still needed. Denkov *et al.*[35,36] succeeded in freezing foam films at various stages of stratification. The electron microscope pictures of such vitrified stratifying films containing latex particles (144 nm in diameter) showed ordered particle arrays of hexagonal packing.[36]

Dushkin *et al.*[37] formed stratifying *wetting* films with latex particles on a solid substrate; after the evaporation of water the dried films were investigated by scanning electron microscopy and atomic force microscopy. The results show that the *hexagonal* packing of the particles is predominant, but there are some narrow regions of *tetragonal* packing. The consecutive formation of hexagonal and tetragonal multilayers was found to follow the phase diagram for a system of spheres confined within a narrow slit (of wedge shape).[38,39] In ref 37 it was found that the type of the lattice (hexagonal or tetragonal) can also be determined by processing the data from interferometric measurements in reflected light. In spite of being "less direct" (as compared to the electron microscopy), this interferometric method has the advantage of giving information about the structuring in *intact* stratifying films (without drying or freezing). Indeed, one cannot completely rule out the possibility that the particle structuring was induced or enhanced in the process of drying or freezing.

That is the reason why in the present study we apply two interferometric methods to investigate *"in vivo"* the structuring in *free* stratifying foam films. Vertical macroscopic films formed in a glass frame from a latex suspension are examined. In section 2 we apply the interferometry at variable *wavelengths*, developed in ref 37. In section 3 we utilize an independent method, the interferometry of the *intensity* reflected from the film. The goal of the study is to experimentally verify whether *hexagonal* particle structuring is present in the free stratifying foam films. This would confirm the theoretical expectations about the type of packing[38,39] as well as the basic statement in the theory of oscillatory structural forces about structuring of particles in narrow slits even when there is no such structuring in the bulk suspension.[22,30−32]

2. Interferometry with Adjustable Wavelength

2.1. Experimental Setup and Materials. The films in our experiments were formed from two types of monodisperse latex suspensions. The first type was *styrene−butadiene* latex (DL-906, DOW) of particle diameter 174 nm, which was measured by us by dynamic light scattering (Malvern 4700C apparatus); the particle concentration was 48 wt %, determined by measuring the weight of a latex sample before and after drying. The second type was *sulfate polystyrene* latex (from IDC) of mean particle diameter 210 nm and particle concentration 30 wt %.

The films were formed in a ring-shape (toroidal) glass frame of inner diameter 1.0 cm (Figure 2). The experimental setup consists of a thermostated table on which a glass beaker with distilled water is situated. The vessel with the sample solution is located in the middle of the glass beaker. The circular glass frame is hanging on a holder. The space around the frame is closed within a glass cell (Figure 2), whose lower part is immersed in the distilled water. In this way the films in the frame are surrounded by saturated vapors and are protected against occasional convective fluxes in the air. By moving the thermostated table upward, the frame can be immersed in the suspension, and then, by moving the table in the opposite direction, the frame can be pulled out from the suspension with a film formed in it. The table is connected

(24) Asakura, S.; Oosawa, F. *J. Chem. Phys.* **1954**, *22*, 1255; *J. Polym. Sci.* **1958,** *33*, 183.
(25) Mitchell, D. T.; Ninham, B. W.; Pailthorpe, B. A. *J. Chem. Soc., Faraday Trans. 2* **1978**, *74*, 1116.
(26) Snook, I. K.; van Megen, W. *J. Chem. Phys.* **1980**, *72*, 2907.
(27) Kjellander, R.; Marçelja, S. *Chem Phys Lett.* **1985,** *120*, 393.
(28) Tarazona, P.; Vicente, L. *Mol. Phys.* **1985,** *56*, 557.
(29) Henderson, D. *J. Colloid Interface Sci.* **1988,** *121*, 486.
(30) Chu, X. L.; Nikolov, A. D.; Wasan, D. T. *Langmuir* **1994**, *10*, 4403.
(31) Chu, X. L.; Nikolov, A. D.; Wasan, D. T. *J. Chem. Phys.* **1995**, *103*, 6653.
(32) Pollard, M. L.; Radke, C. J. *J. Chem. Phys.* **1994**, *101*, 6979.
(33) Kralchevsky, P. A.; Denkov, N. D. *Chem. Phys. Lett.* **1995**, *240*, 385.
(34) Marinova, K. G.; Gurkov, T. D.; Dimitrova, T. D.; Alargova, R. G.; Smith, D. *Langmuir*, submitted.
(35) Denkov, N. D.; Yoshimura, H.; Nagayama, K.; Kouyama, T. *Phys. Rev. Lett.* **1996**, *76*, 2354.
(36) Denkov, N. D.; Yoshimura, H.; Nagayama, K. *Ultramicroscopy* **1996**, *65*, 147.
(37) Dushkin, C. D.; Nagayama, K.; Miwa, T.; Kralchevsky, P. A. *Langmuir* **1993**, *9*, 3695.
(38) Pieranski, P.; Strzelecki, L.; Pansu, B. *Phys. Rev. Lett.* **1983**, *50*, 900.
(39) Pansu, B.; Pieranski, P. *J. Phys.* **1984**, *45*, 331.

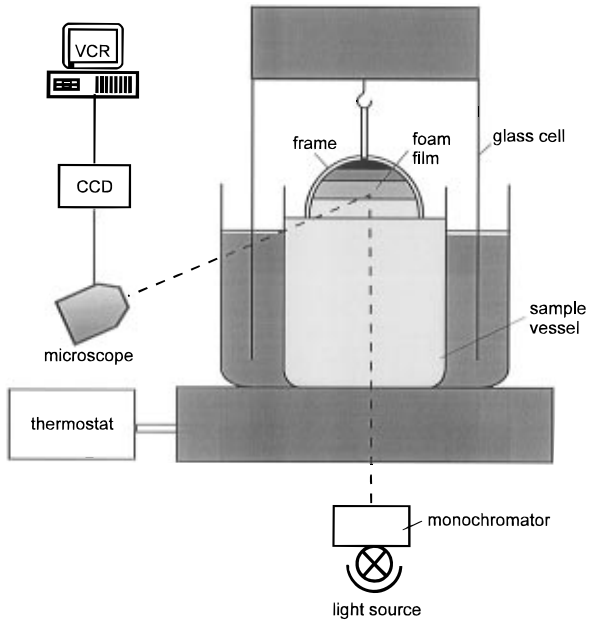

Figure 2. Sketch of the experimental setup. The liquid film is formed in a ring-shaped glass frame. The light reflected from the film is observed by a microscope and recorded by a CCD camera and video-system.

with a thermostat which keeps the temperature constant, 25 ± 0.1 °C, in all experiments.

The evolution of a vertical film thus formed is observed by a horizontal microscope. As a light source we used a monochromator (Monospec 18, Spectrolab, U.K.), which allows to gradually vary the wavelength of the light. The light from the source passes through a collimating optical system and is supplied to the subject by means of an optical fiber. The image of the film is registered by a CCD camera and a video recorder.

After the formation of the film its thickness gradually decreases with time. In polychromatic light one observes the appearance of stripes of various homogeneous colors (and thickness) in the upper part of the frame; i.e., the stepwise profile of the film, shown in Figure 1, develops. As reported in the previous studies, refs 9 and 11, the colors are due to interference of light. In our films with the 174 nm particles we observed in reflected light the following colors (starting from the top of the film): the film without particles is black, the film with one particle layer is ochre, that with two particle layers is blue, that with three layers is yellow, that with four layers is blue, that with five layers is red, and that with six layers is green. Since the color depends on the angle of incidence, in all measurements reported here and hereafter we have used normal incidence.

Looking at the vertical stratifying films, one observes that the boundaries between the stripes are slowly moving downward and the area of the stripes gradually increases. The lower stripes reach the meniscus in the feet of the film and disappear one after another. The area of the upper black stripe without particles increases all the time.

The black films (without particles) formed from the 174 nm suspension were stable, which means that it originally contains surfactant(s) with sufficiently high concentration. In contrast, the black films formed from the original 210 nm suspension were unstable; to stabilize them we added 0.001 M sodium dodecyl sulfate to the 210 nm suspension.

We never observe more than seven or eight homogeneous stratification stripes with the examined latex suspensions. Below, when we speak about hexagonal (or tetragonal) packing of the particles, we always have in mind ordering within this restricted number of uniform stratification stripes, corresponding to relatively thin films. Particle ordering in thicker films, or within the bulk suspension, is not expected.

Table 1. Data for Stripes of Coinciding Intensity (Adjustable Wavelength Method)

k	$\lambda_{k,k+1}$, nm	n_f	m	$f(k)$	$\Lambda(k)$, nm
	(1) Particle Diameter d = 174 nm				
1	524	1.497	3	1	525
2	572	1.510	4	3	758
3	610	1.513	5	5	1008
4	628	1.516	6	7	1243
5	640	1.517	8	9	1688
	(2) Particle Diameter d = 210 nm				
1	494	1.500	4	1	659
2	525	1.514	5	3	867
3	558	1.517	7	5	1287
4	590	1.518	8	7	1554
5	618	1.518	10	9	2035

Our preliminary experiments with larger (visible by optical microscope) polystyrene latex particles showed that the particles are hydrophilic and do not protrude from the liquid surface when captured in a liquid film. Below we assume that the same is true for the much smaller (optically invisible) particles used in the present experiments. In other words, we assume that the particles do not protrude from the film surfaces, as sketched in Figure 1.

2.2. Method of the Adjustable Wavelength. When illuminated with *monochromatic* light, the stripes of different thickness (Figure 1) look like stripes of the same color but of different intensity of brightness. Due to the interference, the brightness (the reflectivity) is a sinusoidal function of the film thickness (see below for details). Therefore, in monochromatic light the stripes look brighter or darker depending on whether they are closer to an interference maximum or minimum.

The method of the adjustable wavelength, developed in ref 37, is based on the observation that when the wavelength of the monochromatic light is varied, the intensities of two neighboring stripes can coincide at a particular wavelength. That is, a special wavelength, $\lambda_{k,k+1}$, exists at which the intensity of the monochromatic light, reflected by two neighboring stripes (containing the k and k+1) particle layers), is the same. Usually for a given couple of stripes there is only one wavelength $\lambda_{k,k+1}$, and the latter can be measured with good precision.

The experimental procedure itself consists of observation of a vertical stratifying film in reflected monochromatic light by means of the horizontal microscope. A couple of neighboring stripes are focused and the wavelength is adjusted by means of the monochromator until the intensities of the two stripes coincide. The respective wavelength, $\lambda_{k,k+1}$, is recorded as a function of k. Since the film drains during the process of observation, for each couple of stripes (for each k) we formed a new film. In this way we succeeded in measuring $\lambda_{k,k+1}$ for all couples of neighboring uniform stripes for both latex suspensions (of particle size 174 and 210 nm). The results are well reproducible. The experimental data for $\lambda_{k,k+1}$ vs k are listed in Table 1.

2.3. Data Interpretation. The interpretation of the data is based on the approach developed in ref 37. Slight modification is necessary, because in our case the film is free (rather than wetting) and the space between the latex particles is occupied by water (rather than air). As noted in ref 37, the reflectivity, R, depends on the film thickness, h, through the phase angle, ψ:[40,41]

(40) Born, M.; Wolf, E. *Principles of Optics*, 4th ed.; Pergamon Press: Oxford, 1970.

$$\psi = \frac{2\pi}{\lambda} h n_f \quad (1)$$

(cf. also eq 16 below). Here λ is the wavelength and n_f is an effective refractive index of the film treated as a continuous medium (for model calculation of n_f, see below). Figure 3 shows schematically the dependence of R on ψ for a free foam film. As seen in Figure 3, a sufficient condition for coincidence of the brightness of two neighboring stripes, $R(\psi_k) = R(\psi_{k+1})$, is

$$m\frac{\pi}{2} - \psi_k = \psi_{k+1} - m\frac{\pi}{2}; \quad \psi_k \equiv \frac{2\pi}{\lambda_{k,k+1}} h_k n_f(k), \quad m = 1, 2, 3, \ldots \quad (2)$$

Here h_k is the thickness of a film containing k particle layers (cf. Figure 1) and we have taken into account that the effective refractive index, n_f, depends on the number of the particle layers, k, inside the film. For even or odd values of m the intensities of the two neighboring stripes will coincide in the vicinity of an interference minimum or maximum, respectively. From eq 2 one can derive[37]

$$m = 2[h_k n_f(k) + h_{k+1} n_f(k+1)]/\lambda_{k,k+1} \quad (3)$$

Following refs 37 and 42 , we will use the empirical dependence of the effective refractive index, n_f, vs the particle volume fraction, φ:

$$n_f(k) = n_p \varphi(k) + n_w[1 - \varphi(k)] \quad (4)$$

where n_p and n_w are the refractive indices of particles and water. For polystyrene n_p is given by the equation[43]

$$n_p = 1.5683 + \frac{1.0087 \times 10^{-10}}{\lambda^2} \quad (5)$$

with λ in centimeters. A monolayer of *hexagonal* close packing can induce formation of a multilayer having a three-dimensional hexagonal close packed (hcp) or face centered cubic (fcc) lattice. In both cases by using geometrical considerations, one deduces[37]

$$\varphi(k) = \frac{\pi k}{3[3^{1/2} + (k-1)2^{1/2}]}, \quad k = 1, 2, 3, \ldots \quad (6)$$

Likewise, a monolayer of square packing can induce formation of a body centered *tetragonal* lattice of *close packing* (tcp), for which

$$\varphi(k) = \frac{\pi k}{3[2 + (k-1)2^{1/2}]}, \quad k = 1, 2, 3, \ldots \quad (7)$$

Values of n_f calculated from eqs 4−6 for a *hexagonal* lattice are listed in Table 1 for various values of k. Note that n_f increases with the increase of k. This means that the increase of n_f with the particle volume fraction, φ, is stronger than the decrease of n_f for growing λ, cf. eq 5.

By means of geometrical considerations (Figure 4) one can conclude that the thickness of a closely packed multilayer can be expressed in the form

$$h_k = d + (k-1)H, \quad k = 1, 2, 3, \ldots \quad (8)$$

where d is the particle diameter. The distance, H, between two neighboring layers (Figure 4) depends on the type of lattice:[37]

$$H = \begin{cases} d(2/3)^{1/2} & \text{for hcp} \\ d/2^{1/2} & \text{for tcp} \end{cases} \quad (9)$$

By using eq 3 (along with eqs 4−9), the data for $\lambda_{k,k+1}$ vs k in Table 1, and the value of d determined by light scattering, one can calculate the order of interference, m, assuming a hcp or tcp lattice. As m must be an integer, we rounded the output of eq 3 to the closest integer number. The values of m, determined in this way for a *hexagonal* lattice, are listed in Table 1. By using eq 8, one can transform eq 3 to read[37]

$$\Lambda(k) = 2d + Hf(k) \quad (10)$$

where

$$\Lambda \equiv \frac{m\lambda_{k,k+1}}{2\bar{n}_f}, \quad \bar{n}_f(k) \equiv \frac{1}{2}[n_f(k) + n_f(k+1)], \quad (11)$$

$$f(k) \equiv \frac{(k-1)n_f(k) + k n_f(k+1)}{\bar{n}_f(k)} \quad (12)$$

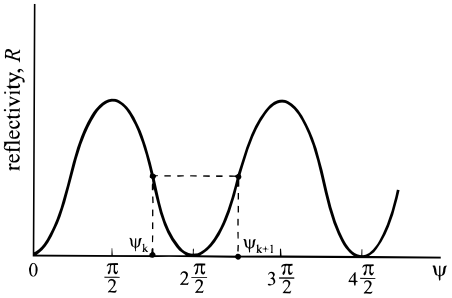

Figure 3. Schematic presentation of the reflectivity, R, of a foam film (in arbitrary units) as a function of the phase angle ψ.

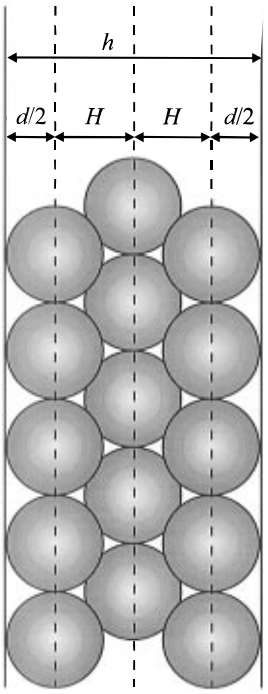

Figure 4. Sketch of a close-packed particle multilayer: d is the particle diameter; H is the distance between the planes of the neighboring particle layers.

(41) Landau, L. D.; Lifshitz, E. M. *Electrodynamics of Continuous Media*; Pergamon Press: Oxford, 1960.
(42) Goodwin, J. W.; Ottewill, R. H.; Parentich, A. *J. Phys. Chem.* **1980**, *84*, 1580.
(43) McDonald, S. A.; Daniels, G. A.; Davidson, J. A. *J. Colloid Interface Sci.* **1977**, *59*, 342.

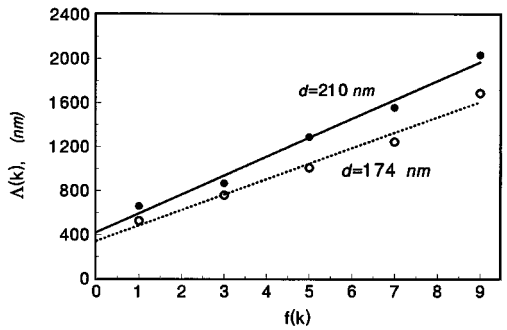

Figure 5. Plot of the data for $\Lambda(k)$ vs $f(k)$ from Table 1 for latex particles of diameters 174 and 210 nm. The linear regressions are drawn in accordance with eqs 9 and 10, the latter for an hcp lattice.

Table 2. Parameters of the Straight Lines for $\Lambda(k)$ vs $f(k)$, Cf. Eqs 10 and 13

d, nm (determined by light scattering)	slope, nm	intercept/slope	correlation coefficient	d, nm (from the intercept)
		hcp Lattice		
174	140 ± 12	2.43 ± 0.52	0.990	171
210	172 ± 12	2.45 ± 0.45	0.992	210
		tcp Lattice		
174	119 ± 0.78	3.47 ± 0.04	0.99994	207
210	158 ± 12	2.19 ± 0.45	0.992	173

$n_f(k)$ is to be calculated from eqs 4−6 or eq 7. The values of $\Lambda(k)$ and $f(k)$ calculated from eqs 11 and 12 for a *hexagonal* lattice (hcp) are shown in Table 1. In accordance with eqs 9 and 10 the plot of $\Lambda(k)$ vs $f(k)$ must be a straight line. In addition, for this line[37]

$$\frac{\text{intercept}}{\text{slope}} = \frac{2d}{H} = \begin{cases} 6^{1/2} & \text{for hcp} \\ 8^{1/2} & \text{for tcp} \end{cases} \qquad (13)$$

Our data for $\Lambda(k)$ vs $f(k)$ for an *hcp lattice* are plotted in Figure 5. One sees that the data agree well with a straight line. The parameters of the linear regressions, listed in Table 2, show that for both straight lines the ratio intercept/slope is very close to $6^{1/2} = 2.45$ and noticeably less than $8^{1/2} = 2.83$. The correlation coefficient given in Table 2 is the standard characteristics of the quality of the fit used in the linear regression analysis. The experimental error is considerable, which is a consequence of the dynamic character of the measurements with our draining free vertical films. Nevertheless, the mean values of the diameter, d, independently determined from the slope and intercept of the linear regressions in Figure 5 (see eqs 9 and 10), are very close to each other and to the particle diameter determined by light scattering (Table 2). From this viewpoint, the results are very well consistent with the hypothesis for the presence of an *hcp lattice* within the film. As discussed below, this is not the case if we try to interpret the data by means of the hypothesis for the presence of a *tcp lattice* within the film.

For the sake of comparison we tried to fit the same data for $\lambda_{k,k+1}$ vs k with the equations stemming from the hypothesis that the lattice is *tetragonal*. For this purpose we calculated $\Lambda(k)$ vs $f(k)$ for a *tcp lattice*; the calculations are similar to those for an hcp lattice, but eq 7 is used instead of eq 6. The plot of $\Lambda(k)$ vs $f(k)$ for a tcp lattice also agrees well with a straight line (see the correlation coefficients in Table 2). However, the ratio of the intercept to the slope (which is 3.47 ± 0.04 for the 174 nm particles and 2.19 ± 0.45 for the 210 particles) is markedly different from the value $8^{1/2} = 2.83$ corresponding to a tcp lattice. The values of the diameter, d, independently determined from the slope and intercept of the linear regressions (168 and 207 nm for the 174 nm particles and 224 and 173 nm for the 210 particles) are very different from each other: From this viewpoint, the results are not consistent with the hypothesis for the presence of a *tcp lattice* within the film. The very good correlation coefficient in the case of the 174 nm particles (Table 2) seems to be occasional.

Equation 8 and Figure 4 are based on the model assumption about close packing of the particles within the investigated stratifying films. As seen, such an assumption agrees with the experimental data (Table 2). This fact might be attributed to the overlap of the structured zones in close vicinity to the two film surfaces.[22] As already mentioned, particle ordering in thicker films, or within the bulk suspension, is not expected.

In summary we can conclude that the method of the adjustable wavelength is sensitive enough to distinguish between two types of particle packing inside a stratifying film. The fulfillment of the criterion given by eq 13 implies that the interferometric data for $\lambda_{k,k+1}$ are in agreement with a *hexagonal* rather than a tetragonal lattice. Similar results are obtained in ref 37 for dried wetting films with latex particles on a solid substrate. The experimental precision in our case is worse than that in ref 37, most probably due to the dynamic character of the measurements with our draining free films.

As demonstrated below, the application of an independent and alternative interferometric method to the same vertical stratifying films confirms the conclusion about the hexagonal packing of the particles within such films.

3. Interferometry of the Reflected Intensity

3.1. Experimental Method. As found in the previous section, the type of the lattice affects the interferometric data mostly through the quantity H in eq 9. Note that H determines the slope of the line h_k vs $k - 1$ in eq 8. In fact, one can measure h_k from the *intensity* of the *monochromatic* light reflected from the film by means of a classical interferometric method.[18,44,45] It is based on the following relation between the film thickness, h, and the intensity of the reflected light, I:

$$h = \frac{\lambda}{2\pi n_f}\left[m\pi \pm \arcsin\sqrt{\frac{\Delta}{1 + 4Q(1-\Delta)/(1-Q)^2}}\right] \qquad (14)$$

where

$$\Delta \equiv \frac{I - I_{min}}{I_{max} - I_{min}}, \quad Q \equiv \left(\frac{n_f - 1}{n_f + 1}\right)^2 \qquad (15)$$

Here I_{max} and I_{min} are the values of I corresponding to the interference maximum and minimum and m denotes the order of interference. As the stripes in our case correspond to various orders of interference, it is convenient to invert eq 14:

$$\Delta I(h) = \frac{(1+\beta)\Delta I_{max}}{1 + \beta \sin^2(2\pi n_f h/\lambda)} \sin^2(2\pi n_f h/\lambda), \qquad \beta \equiv \frac{4Q}{(1-Q)^2} \qquad (16)$$

$$\Delta I(h) \equiv I(h) - I_{min}, \quad \Delta I_{max} \equiv I_{max} - I_{min} \qquad (17)$$

($\beta \approx 0.185$ accounts for the multiple reflection between the two film surfaces). In our experiments I_{min} is measured as the intensity of the light in the absence of a film in the

(44) Vasicek, A. *Optics of Thin Films*; North Holland Publishing Co.: Amsterdam, 1960, p 60.
(45) Scheludko, A. *Kolloid-Z.* **1957**, *155*, 39.

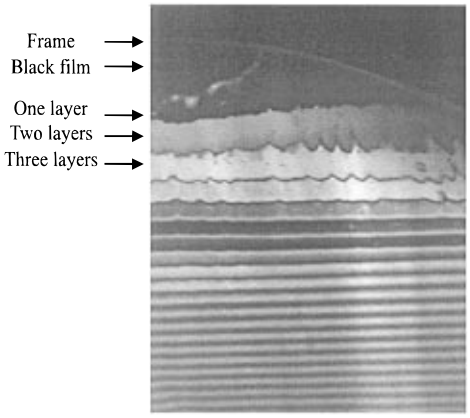

Figure 6. Photograph of a stratifying vertical foam film in reflected light. Stripes of uniform thickness, containing from one up to 7 layers of latex particles (diameter 174 nm), are observed in the upper part of the picture. Under the stripes one sees the interference fringes from the Plateau border beneath the film (Figure 1).

frame (after rupturing of the film). On the other hand, because of the stepwise character of film thinning it is not possible to determine ΔI_{max} with a good precision; for that reason when processing the experimental data ΔI_{max} is treated as an adjustable parameter, which scales the sinusoidal dependence given by eq 16.

In our experiments we measured the intensities, ΔI_k, of the stripes, containing k layers of particles, $k = 1, 2, 3, ...$; cf. Figure 1. To check whether the data agree with the hypothesis about the presence of *hexagonal* or *tetragonal* packing of the particles within the film, we used eq 8 (along with eq 9) to calculate h_k. As in this case the calculated $\Delta I(h)$ is not very sensitive to the value of the film refractive index; we took an average value, $n_f = 1.511$, corresponding to the 174 nm particles. To fit the data for ΔI_k vs k by means of the least squares method, we numerically minimized the function

$$\Phi(\Delta I_{max}, d) = \sum_{k=1}^{n} [\Delta I_k - \Delta I(h_k)]^2 \qquad (18)$$

where the function $\Delta I(h_k)$ is determined from eqs 8 and 16 for $h = h_k$. The values of ΔI_{max} and d are determined from the best fit as adjustable parameters.

3.2. Measurements and Data Processing. Experimentally we recorded the process of stepwise drainage of vertical foam films by means of the video-system (Figure 2). Measurements with one type of latex particles, that of diameter $d = 174$ nm, were carried out at two wavelengths: $\lambda = 540$ and 640 nm. In this case we used a stabilized source of polychromatic light with appropriate interference filters. A video-frame taken at $\lambda = 540$ nm is reproduced in Figure 6. The uniform stripes in the upper part of the picture are due to the stepwise profile of the film in this zone (see also Figure 1). The consecutive maxima and minima of the light intensity in the lower part of the picture (Figure 6) are due to the interference of the light beams reflected from the two smooth surfaces of the Plateau border beneath the film.

As the vertical film is draining, all the stripes are *moving* downward with time. Therefore, if one focuses at a given point and measures the intensity of the reflected light there, it is observed that the intensity is varying with time, since interference fringes of various intensity are passing through the field of observation. This varying intensity was recorded by us by means of the video-system, and then the signal was digitized and stored in a computer. Figure 7 shows a typical record of the intensity, I, vs time for $\lambda = 540$ nm. The oscillatory curve on the left

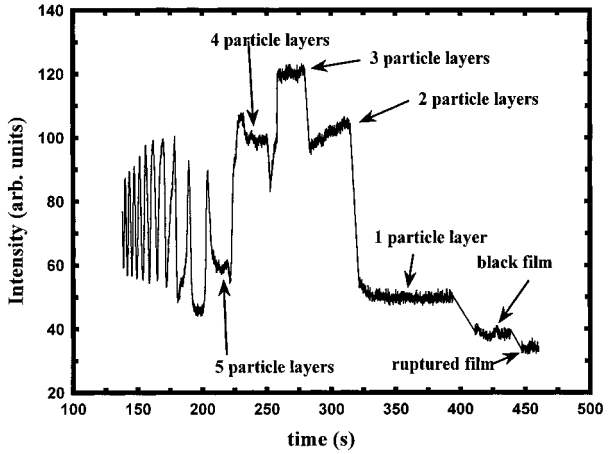

Figure 7. Plot of intensity, I, of the reflected light vs time: a typical experimental interferogram from a vertical stratifying film containing latex particles ($d = 174$ nm; $\lambda = 540$ nm).

Table 3. Data for the Intensity, $\Delta I_k \equiv I_k - I_{min}$, of the Light Reflected from the Stratification Steps Containing k Particle Layers for Two Wavelengths λ

k (number of particle layers)	ΔI_k ($\lambda = 540$ nm)	ΔI_k ($\lambda = 640$ nm)
1	16.0 ± 1.4	53.1 ± 2.4
2	67.1 ± 2.6	94.9 ± 9.5
3	86.1 ± 1.2	36.3 ± 4.2
4	64.6 ± 4.9	16.8 ± 2.7
5	25.8 ± 2.1	88.2 ± 3.4
6	12.2 ± 1.2	16.7 ± 2.6
7	21.4 ± 4.3	

corresponds to the image from the Plateau border in the lower part of Figure 6. The stratification stripes appear as deviations from smooth oscillatory behavior of the curve in Figure 7. One can see that the signal from the stratification steps is affected by some stochastic noise in the system, which fortunately is relatively low. The thickness of some of the steps (like that containing two particle layers in Figure 7) is decreasing with time, which is manifested by the fact that the step in the interferogram is not horizontal.

As mentioned above, the interferograms, like that in Figure 7, are available in digital form. We processed by computer each portion, corresponding to a stratification step on a given curve, and calculated the average intensity, I_k, and the standard deviation of its value. In the same way, I_{min} was obtained from the intensity corresponding to a ruptured film (Figure 7). Then $\Delta I_k \equiv I_k - I_{min}$ was determined. The data for ΔI_k (in arbitrary units) vs k obtained in this way for the two wavelengths are listed in Table 3.

Next, the data in Table 3 were processed by means of the least squares method based on eqs 16−18. The best fits, shown in Figure 8, present ΔI as a function of the film thickness h. The continuous oscillatory line represents the output of eq 16 under the assumption of *hexagonal* packing of the particles, whereas the black dots represent the experimental points from Table 3. In particular, the curve in Figure 8a corresponds to the photograph at $\lambda =$ 540 nm shown in Figure 6. One sees that when two neighboring experimental points in Figure 8a are separated by an interference *minimum*, the boundary between the respective stripes in Figure 6 looks *dark*. And *vice versa*, a *bright* boundary between two stripes in Figure 6 corresponds to two experimental points separated by an interference *maximum* in Figure 8a. The situation with the data in Figure 8b, corresponding to $\lambda = 640$ nm, is quite similar with the only difference being that the period of the oscillatory curve is greater than that in Figure 8a because of the longer wavelength.

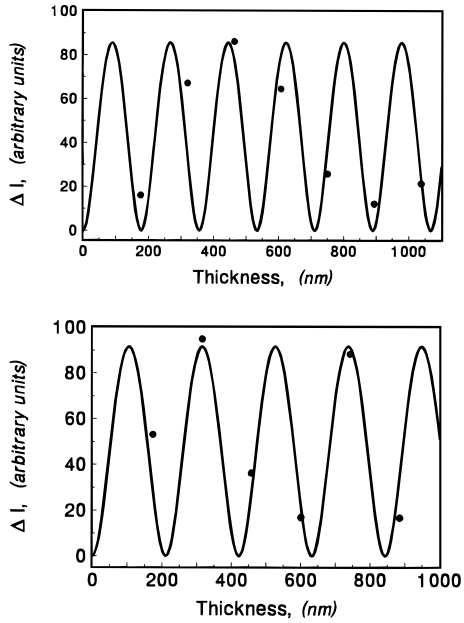

Figure 8. Plot of the intensity of the reflected light, ΔI, vs the film thickness, h: comparison of the experimental data from Table 3 (the dots) with the best fit obtained by eqs 16−18 (the oscillatory line) for wavelengths (a, top) $\lambda = 540$ nm and (b, bottom) $\lambda = 640$ nm.

Table 4. Parameters of the Fits of the Data in Table 3 by Means of Eq 16

λ, nm	d, nm (from the best fit by eq 16)	$\delta(\Delta I)/\Delta I_{max}$
	hcp Lattice	
540	174.3	0.193
640	174.1	0.159
	tcp Lattice	
540	194.5	0.303
640	191.7	0.223

As already mentioned, the values of ΔI_{max} and d are determined from the best fit as adjustable parameters. If the value of d thus determined is close to the known particle diameter (obtained by dynamic light scattering), this would mean that the data are consistent with the model of hexagonal (or tetragonal) packing of the particles within the film. The assumption about the type of packing is incorporated in eq 8, the latter being a part of the calculation scheme of $\Delta I(h_k)$, see eq 18.

Table 4 contains the parameters of the fits of the data in Table 3 by means of eqs 16−18 for hcp and tcp lattices. To characterize the fits, we use the "standard deviation" of the intensity defined as follows:

$$\delta(\Delta I) = [\Phi_{min}/(n - 1)]^{1/2} \qquad (19)$$

where Φ_{min} denotes the minimum value of Φ in eq 18 and n is the number of experimental points in Table 3. One sees that, assuming an *hcp lattice*, we obtain the real diameter of the latex particles, $d = 174$ nm, determined independently by light scattering. This is true for the two wavelengths used, $\lambda = 540$ and 640 nm, see Table 4.

In contrast, assuming a *tcp lattice* from the best fit, we obtain values of d which are noticeably greater than the real value, 174 nm, see Table 4. Moreover, the fits with an hcp lattice are better than those with a tcp lattice, which is evidenced by the smaller values of Φ_{min} and $\delta(\Delta I)$ in the case of an hcp lattice for one and the same set of processed experimental data, see eq 19 and Table 4.

These results lead to the conclusion that the interferometry of the reflected intensity is sensitive to the type of particle packing inside the stratifying film and show that the packing of the particles is hexagonal.

Finally, it should be noted that the interferometry of the reflected intensity can be applied to study the structuring of smaller colloidal particles (such as surfactant micelles or protein globules) in stratifying films. The only limitation of this method is the requirement that the height of the stratification steps be larger than the stochastic noise (cf. Figure 7), which introduces an error of ca. ±1 nm in the value of the measured thickness, h. In contrast, the interferometry with adjustable wavelength (see section 2 above) cannot be applied to stratifying films containing *very small* colloidal particles, when all stepwise transitions are observed on the left of the last interference maximum in Figure 3 ($\psi < \pi/2$, $h < \lambda/4n_f$); cf. eq 1.

4. Concluding Remarks

In the present article we apply two independent interference methods to establish the type of packing of the latex particles contained within a vertical stratifying film, cf. Figure 1. The films are formed in a ring-shaped frame, after its pulling out of the latex suspension (Figure 2). The stratifying films exhibit a stepwise profile, which appears as a set of parallel stripes of uniform intensity varying from stripe to stripe. The first interference method is based on wavelength measurements, whereas the second one is based on intensity measurements. Both of them allow a study of the stratification phenomenon "*in vivo*", i.e. during the process of film drainage.

The *interferometry with adjustable wavelength* gives the value of the light wavelengths, for which the intensities of the various couples of neighboring stratification stripes coincide, see Table 1. Then the data are fitted with a straight line in accordance with eq 10. The slope and the intercept of the linear regression (see Figure 5, Table 2, and eq 13) evidence that the particle packing within the film is hexagonal.

The *interferometry of the reflected intensity* gives the intensity of the stratification stripes as a function of the number of particle layers within the film, see Table 3. To fit the data with eq 16, we vary the particle diameter as an adjustable parameter. The value of the diameter corresponding to the best fit is then compared with the known particle diameter determined by the dynamic light scattering method.

To fit the data from each of these two methods, we assume a given type of particle packing, in our case hexagonal or tetragonal, and check which type is consistent with the data. In all cases the data indicate the presence of *hexagonal* packing and do not agree with tetragonal packing. The interference methods used by us are not able to distinguish between lattices of very close particle volume fraction, like cubic face centered and hexagonal.

In spite of being indirect, the interference methods used by us give information about the type of particle structuring in *intact* stratifying films, during the process of their drainage. The study of intact films is not accessible to such a direct method as cryoelectron microscopy,[35,36] which examines frozen films. We hope that the interference methods used in the present study, and especially the interferometry of the reflected intensity, can be successfully applied to investigate the particle structuring of much thinner stratifying films containing surfactant micelles or protein globules.

Acknowledgment. This work was supported by the National Science Fund of Bulgaria. The authors are indebted to Mr. Dobrin Bossev for his help in the interferometric measurements.

LA970145S